On the Recycling of Random FM Radar Waveforms

Thomas J. Kramer, Jonathan W. Owen, Matthew B. Heintzelman, Shannon D. Blunt
Radar Systems Lab (RSL), University of Kansas, Lawrence, KS

***Abstract*—Random frequency modulated (RFM) waveforms have been found to possess a number of useful radar properties such as high dimensionality, good spectral containment, and amenability to high-power transmitters. Moreover, RFM waveforms can be optimized according to a desired spectral template and/or to obtain relatively low range sidelobes. Here we examine a way to greatly reduce the need for the optimization/ storage of new waveforms by performing "recycling" of existing waveforms that have already been optimized. It is shown via hardware loopback capture that recycled versions can largely preserve characteristics of the original while still producing sufficiently distinct new waveforms.**

Keywords—frequency modulation, optimization, noise radar, waveform diversity

I. Introduction

There is a growing body of work regarding the design and generation of RFM waveforms and subsequent applications [1-3]. The key benefits of such waveforms are their high dimensionality, which arises from their nonrepeating nature, and the constant-amplitude/continuous-phase structure inherent to FM that makes them suitable for high-power transmitters. Further, recent efforts seeking to impose useful spectrum shaping also provide better containment to address mounting congestion while likewise reducing range sidelobes by virtue of the Fourier relationship between the spectral density and autocorrelation [3].

When slow-time processing is performed across a set of RFM waveforms after pulse compression, the unique pulse-to-pulse range sidelobe structure realizes an incoherent averaging effect. Since the mainlobes remain coherent, an additional sidelobe suppression factor of M (for M unique waveforms) is thereby achieved. Of course, the trade-off for this effect is nonstationarity in the form of range sidelobe modulation (RSM) [3] that, at least when time-bandwidth product (TB) and/or the number of pulses is modest, may necessitate some manner of receive compensation depending on the application (e.g. [4]).

It has been found that RFM waveform formulations can be loosely categorized into one of three classes: *a*) those requiring per-pulse optimization (e.g. [5-7]), *b*) those requiring offline optimization followed by random generation [8], and *c*) those constructed in a manner that requires no optimization at all [9,10]. The trade-off between classes is computational cost versus performance (or spectral control). In [11] it was shown how a collection of well-designed waveforms could be reused to address computational/memory limitations, subsequently yielding another trade-off in terms of the concentration (or diffusion) of subsequent RSM.

Here, we explore another approach to reusing previously generated waveforms, or at least attributes thereof, as a means to avoid the design and storage of new instantiations. Specifically, the notion of "recycling" is proposed whereby segments of a waveform's instantaneous frequency function are randomly permuted so that the ensuing instantaneous phase function is sufficiently unique yet possesses much of the same general attributes as the original. It is shown that a substantial number of new and useful RFM waveforms can be produced in this manner.

II. Waveform Recycling

The idea of reassembling a new FM waveform from an existing one can be traced back to Costas coding [12] in which a set of spectral components are rearranged in time (see Fig. 1). This general idea has since been examined extensively (e.g. [13-18]) and has been extended to facilitate Sudoku-based waveforms [19], a form of dual-function radar/ communications [20], and MIMO radar/sonar [21-24]. In contrast, we aim to produce as many new diversified waveforms as possible for use in the context of nonrepeating RFM applications (e.g. see [3] and references therein).

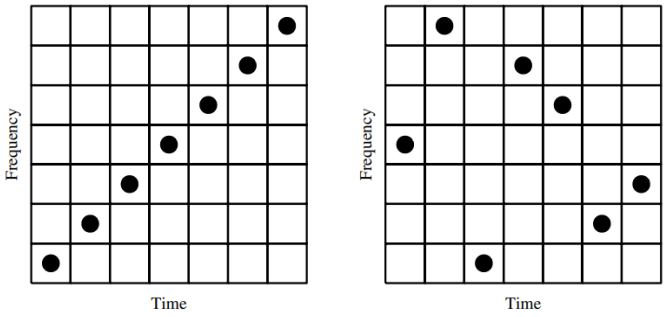

Fig. 1: Comparison of linear (left) and Costas (right) coding matrices

Specifically, we consider the decomposition and subsequent rearranging of an arbitrary FM waveform in a manner that avoids the need for any further optimization, largely retains the general characteristics of the original, and preserves phase continuity so that minimal transmitter distortion is maintained. Let

$$\begin{aligned} s(t) &= \exp\left(j2\pi \int_0^t f(\tau)\, d\tau \right) \\ &= \exp\big(j2\pi \phi(t) \big) \end{aligned} \tag{1}$$

be an arbitrary FM waveform having temporal extent T, where the integration of instantaneous frequency function $f(\tau)$ in the top line ensures $\phi(t)$ is a continuous phase function in the bottom line. It is then rather straightforward to divide the frequency function into M non-overlapping segments denoted $f_1(\tau)$, $f_2(\tau)$, $\cdots$, $f_M(\tau)$, where each segment has the same

This work was supported by the Office of Naval Research under Contract #N00014-20-C-1006. DISTRIBUTION STATEMENT A. Approved for Public Release.
978-1-6654-8278-3/23/$31.00 ©2023 IEEE

temporal extent $T_{\text{seg}} = T/M$. From these segments it is then possible to assemble $M!$ different waveform permutations, with '!' denoting the factorial operation. While we shall fix the same T_{seg} for all segments, note that differing lengths is also possible.

In terms of these segments, the original waveform can be expressed as

$$f(\tau) = \sum_{m=1}^{M} f_m\left(\tau - (m-1)T_{\text{seg}}\right). \tag{2}$$

Now let the operator $P\{1, 2, \ldots, M\}$ produce a permuted ordering of the set of segment indices, such that index $p_m \in \{1, 2, \ldots, M\}$ denotes the mth order-permuted element. Since each segment could be time-reversed without altering the aggregate spectral content, we can therefore define

$$\bar{f}_m(\tau) = \begin{cases} f_m(\tau) & \text{with prob. } \tfrac{1}{2} \\ f_m(T_{\text{seg}} - \tau) & \text{with prob. } \tfrac{1}{2} \end{cases} \tag{3}$$

for each of the $m = 1, 2, \cdots, M$ segments. Moreover, a random sign-change could also be imposed via

$$\bar{f}_m(\tau) = \begin{cases} f_m(\tau) & \text{with prob. } \tfrac{1}{4} \\ f_m(T_{\text{seg}} - \tau) & \text{with prob. } \tfrac{1}{4} \\ -f_m(\tau) & \text{with prob. } \tfrac{1}{4} \\ -f_m(T_{\text{seg}} - \tau) & \text{with prob. } \tfrac{1}{4} \end{cases}, \tag{4}$$

though doing so no longer truly preserves the aggregate spectral content of the original waveform (but does serve to further expand the set of possible new waveforms).

Using either (3) or (4), collecting the resulting segments like in (2) yields the new instantaneous frequency function

$$\tilde{f}(\tau) = \sum_{m=1}^{M} \bar{f}_m\left(\tau - (p_m - 1)T_{\text{seg}}\right), \tag{5}$$

where permuted index p_m has replaced the original index m, subsequently providing the new recycled waveform

$$\begin{aligned} \tilde{s}(t) &= \exp\left(j2\pi \int_0^t \tilde{f}(\tau)\, d\tau\right) \\ &= \exp\left(j2\pi \tilde{\phi}(t)\right) \end{aligned}. \tag{6}$$

The presence of the integration stage in (1) and (6) ensures that the ensuing phase is a continuous function of time, since discontinuities would otherwise produce undesired spectral spreading that ultimately translates to increased transmitter distortion [25]. Based on (3), each recycled waveform possesses the same frequency content versus time as the original waveform, albeit reordered and intermittently time-reversed (segment-wise). Consequently, the spectral density is expected to be nearly identical to the original waveform via the principle of stationary phase (PSP) [26]. Discontinuities in the recycled instantaneous frequency function of (5) are the reason why the original and recycled spectral densities are not identical, with the difference observed as a modest broadening in the roll-off region.

In the case that sign-changed segments are employed via (4), the per-waveform spectral content does actually change, though on average (across a set of recycled waveforms) it is largely expected to conform to that of the original waveform. A notable exception lies in the case of spectral notching which, as demonstrated in [27], is due to a cancellation effect as opposed to being a result of PSP since RFM waveforms do not possess monotonicity in their frequency function. Generally, most symmetric spectrum waveforms will conform spectrally even on a pulse-by-pulse basis. However, waveforms with little to no variation in chirp rate should not use sign change, as this can substantially alter the center frequency and bandwidth of these waveforms.

The inclusion of random time-reversed and sign-changed versions of segments per (4) means that the number of possible recycled waveforms is $(M!)\,4^M$, which as shown in Fig. 2 exceeds 10^M for $M \geq 5$. In short, while it is certainly possible to randomly realize an identical span of a few segments that would produce a similar waveform (and therefore not achieve the same degree of uniqueness as other RFM methods), the actual likelihood of doing so for a given coherent processing interval (CPI) comprised of a few hundred or even a few thousand recycled waveforms is vanishingly small as M grows beyond modest values. Thus, while simple in concept, waveform recycling leads to some interesting attributes that we explore in the next section.

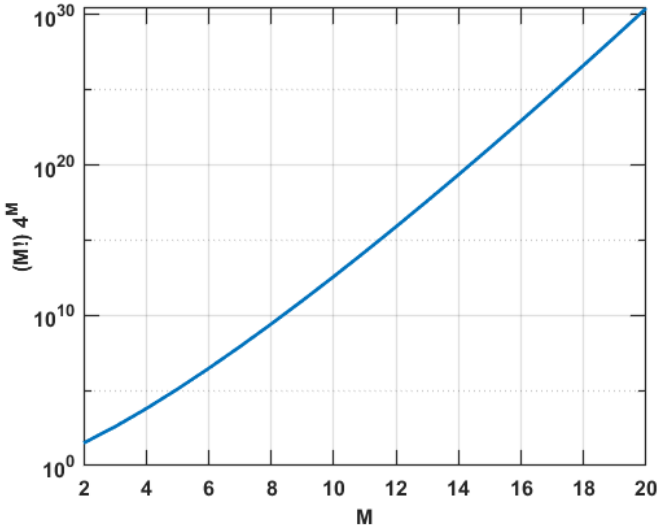

Fig. 2: Number of possible recycled waveforms vs. number of segments *M*

III. Assessment of Waveform Recycling

To demonstrate the efficacy of waveform recycling, different degrees of segmentation were examined in terms of spectral shape/containment, autocorrelation response after coherent combining, and impact to spectral transmit notching. In each case, 10^3 recycled waveforms were generated from a single baseline waveform that was designed via the PRO-FM method [5] to match a Gaussian power spectral density (PSD). This waveform has TB = 300 and the discretized form is oversampling by a factor of 3 relative to 3-dB bandwidth.

Three different segmentation regimes were then considered, with M set to 4, 20, and 100. Relative to the total TB of 300, these regimes correspond to the individual segments having dimensionality $T_{\text{seg}}B$ = 75, 15, and 5, respectively. In other words, since longer segments preserve more structure from the

original waveform, these regimes illustrate the trade-off between greater diversity (higher M, as suggested by Fig. 2) and maintaining properties for which the original waveform was designed (e.g. spectral notches).

Fig. 3 illustrates the PSD of the baseline PRO-FM waveform along with the Gaussian PSD template. A single FM waveform cannot perfectly match the template since it does not possess amplitude modulated (AM) degrees of freedom. However, the given optimized waveform does conform fairly well, with only minor spectral broadening at the band edges.

A spectrally notched version of the Gaussian template and PSD of a subsequent PRO-FM baseline waveform are shown in Fig. 4. The need for a symmetric notch arises from the use of the sign-change version of recycling from (4), where asymmetric notches would instead require (3) that only permits time-reversal.

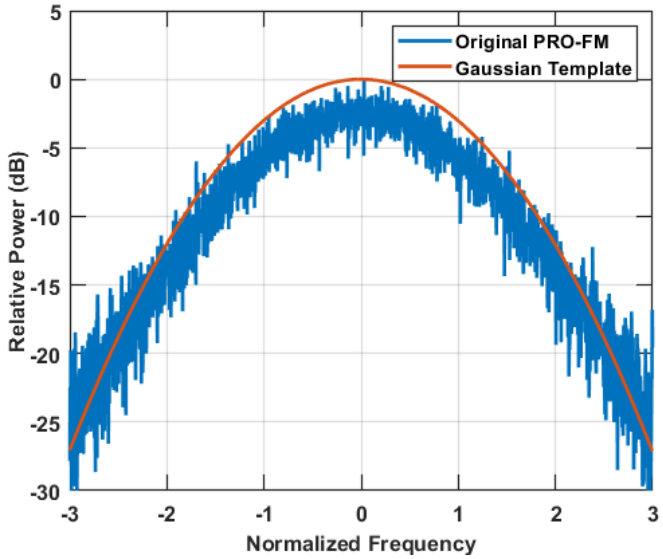

Fig 3: Baseline PRO-FM waveform and Gaussian template

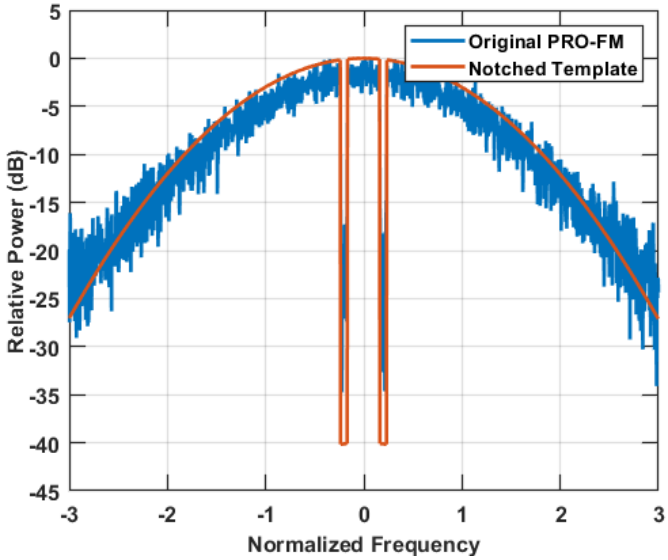

Fig 4: Baseline PRO-FM waveform and symmetrically-notched Gaussian template

For the 10^3 recycled waveforms generated for each segmentation regime the mean PSD was computed, which is plotted in Fig. 5 along with the initial Gaussian template. We see that as M increases, the aggregate PSD becomes smoother (i.e. recycled waveforms become more unique, hence improved averaging). The trade-off for this effect is a more gradual roll-off at the band edges (i.e. modest spectral containment degradation).

If spectral notches are present in the baseline waveform, notch depth clearly degrades with increasing M, as depicted in Fig. 6. Specifically, compared to the original notched PSD in Fig. 4, the M = 4 and 20 cases yield about 15 dB and 23 dB degradation in notch depth, respectively, while the M = 100 case has lost the notches entirely.

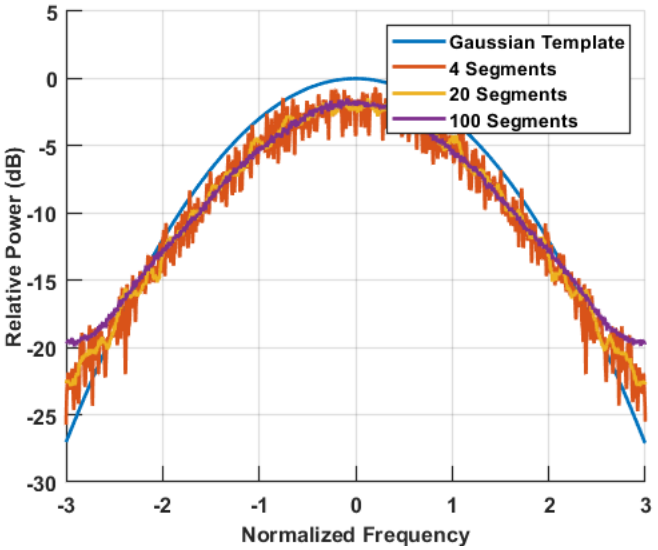

Fig 5: Mean PSD for the set of 10^3 recycled waveforms produced by each segmentation regime for a Gaussian PSD template

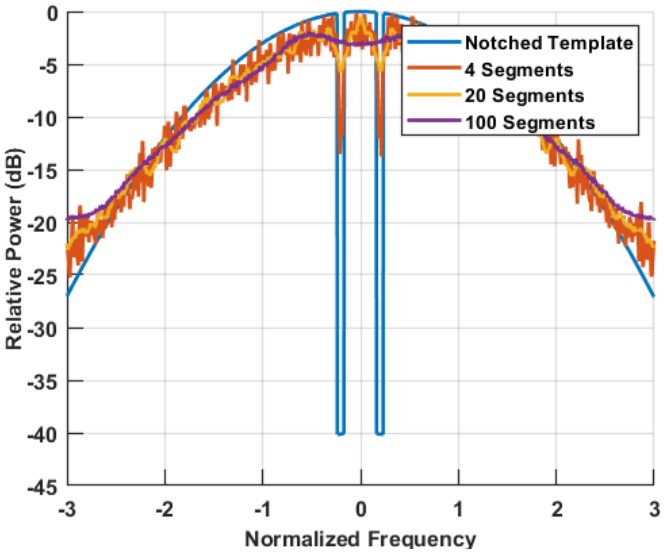

Fig 6: Mean PSD for the set of 10^3 recycled waveforms produced by each segmentation regime for symmetric spectral notches

In the notched waveforms shown in Fig. 6, the notches were symmetric about center frequency. Fig. 7 shows a case with an asymmetric notch on the left side of the spectrum but is recycled using the method in (3) rather than (4). If negation was included such as used in (4), the resulting waveform spectrum would resemble that of Fig. 6, with a less deep notch formed in two symmetric spectral locations. Notably, the notch is clearly deeper in the asymmetric case (about 5 dB), which is actually due to the optimization method used to obtain the initial waveform, since it is easier to form one deep notch than two [5]. Other methods may allow the notch depth to be more heavily weighted, with a penalty to the rest of the spectrum.

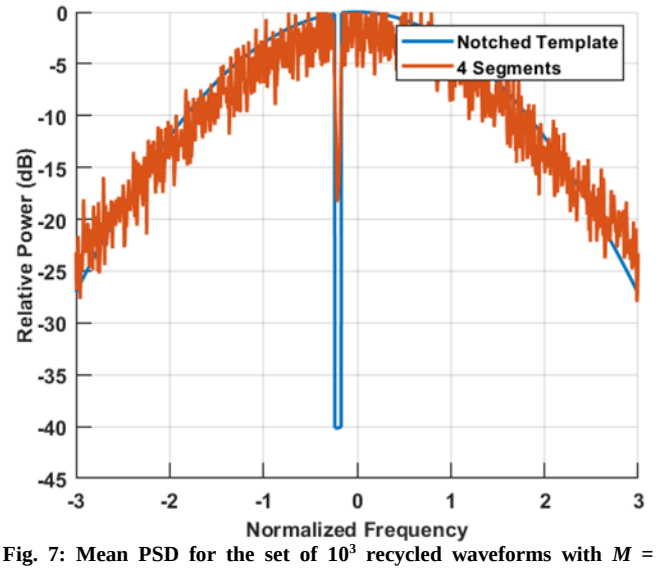

Fig. 7: Mean PSD for the set of 10^3 recycled waveforms with M = 4 segments for an asymmetric spectral notch.

Figs. 8-10 show both a single waveform autocorrelation and the coherently combined response (i.e. zero-Doppler response after slow-time processing) for 4, 20, and 100 segments, respectively. The single waveform autocorrelation in each case is essentially the same, which makes sense given that each is a single recycled instantiation of the baseline PRO-FM. However, a rather different response is observed when coherent combining is performed. Because changing M from 4 to 20 to 100 introduces greater uniqueness, the latter (Fig. 10) reveals a response that is qualitatively the same as what is obtained from combining completely independent RFM waveforms (see [3]), achieving $10\log(10^3) = 30$ dB of incoherent sidelobe averaging suppression. The M = 20 case (Fig. 9) is somewhat similar, albeit with the appearance of near-in shoulder lobes causes by a bit less independence across the set of 1000 recycled waveforms. It is therefore unsurprising that this degradation in independence is notably greater for the M = 4 case (Fig. 8).

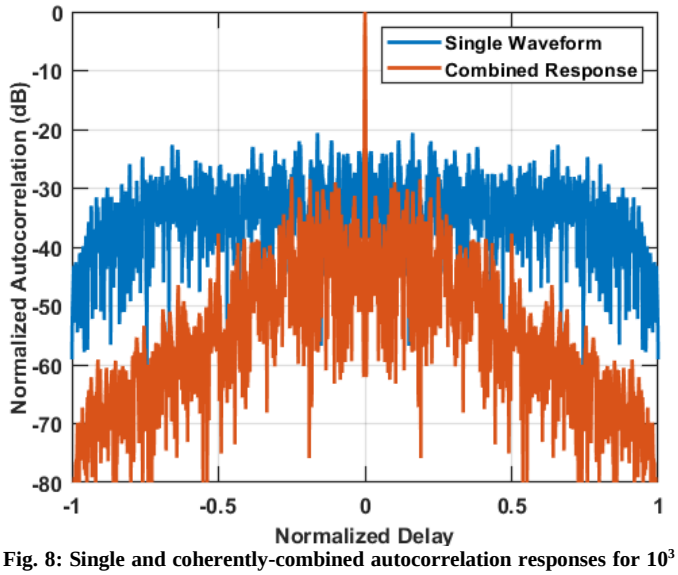

Fig. 8: Single and coherently-combined autocorrelation responses for 10^3 waveforms recycled using $M = 4$ segments

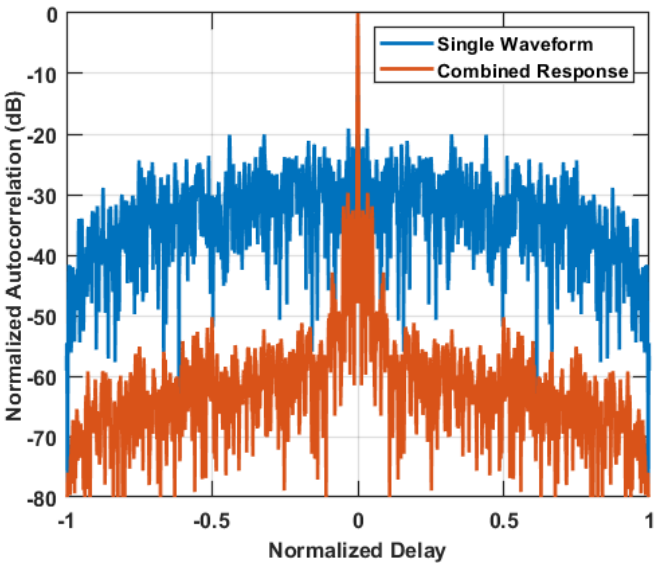

Fig. 9: Single and coherently-combined autocorrelation responses for 10^3 waveforms recycled using $M = 20$ segments

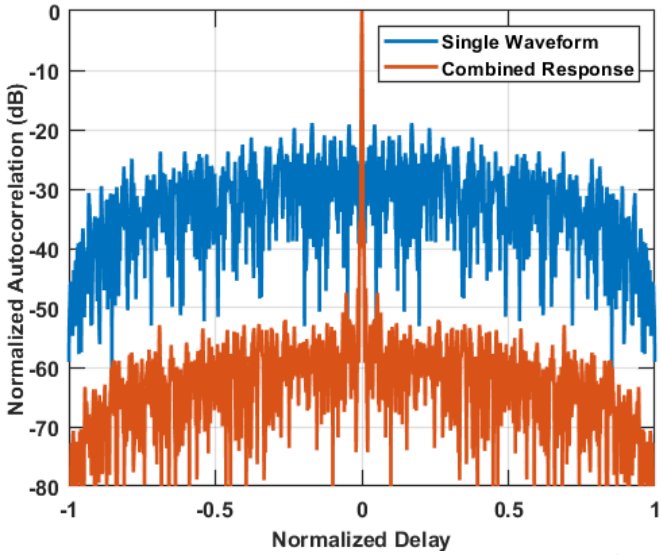

Fig. 10: Single and coherently-combined autocorrelation responses for 10^3 waveforms recycled using $M = 100$ segments

IV. Loopback Measurements

To experimentally demonstrate the utility and trade-space of recycling, loopback measurements of the three waveform sets were collected using a 3-dB bandwidth of 66.6 MHz and oversampled by a factor of 3. The waveforms were produced by an arbitrary waveform generator (AWG) at a center frequency of 3.45 GHz and captured using a real-time spectrum analyzer.

Fig. 11 shows the mean PSD of each waveform set. While the same degree of variation is present (smoother for higher M), the roll-off behavior is now altered by the analysis bandwidth of the spectrum analyzer. Fig. 12 likewise depicts the coherently combined autocorrelation response for each waveform set, which clearly agrees with Figs. 8-10.

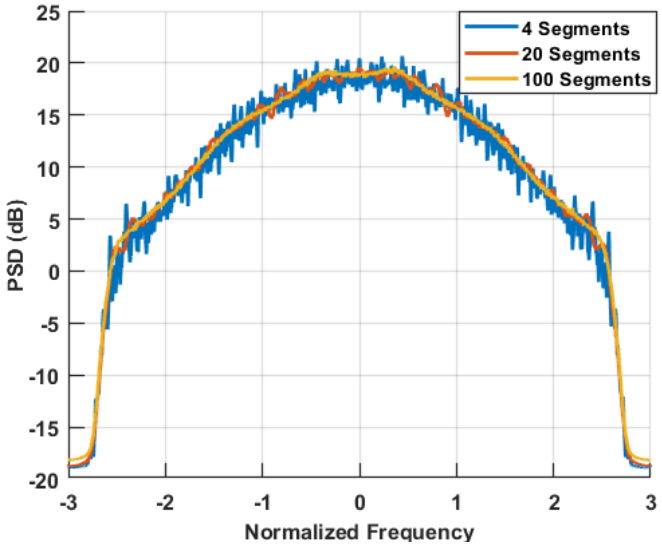

Fig. 11: Mean PSD for the set of 10^3 recycled waveforms produced by each segmentation regime for a Gaussian PSD template and loopback captured

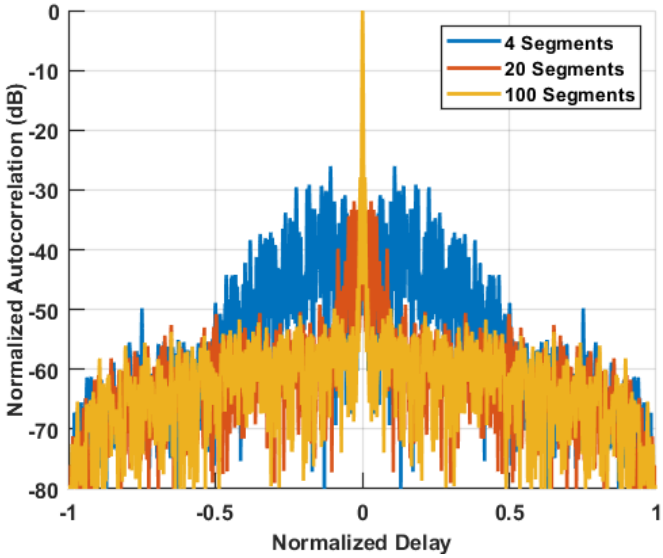

Fig. 12: Coherently-combined autocorrelation responses for 10^3 waveforms recycled via $M = 4$, 20 and 100 segments and loopback captured

V. Conclusions

Recycling provides a way to synthesize new RFM waveforms from an existing optimized structure based on some specified degree of segmentation, along with time-reversal and possible sign-changing of segments. This approach therefore reduces computational cost and/or storage requirements. There are, of course, trade-offs in performance with regard to independence across the recycled waveform set, achievable spectral notch depth (if relevant), and spectral roll-off at the band edges. Future work will consider the use of recycled waveforms as initializations for waveform optimizations like those used in [6].

References

[1] S.R.J. Axelsson, "Noise radar using random phase and frequency modulation," *IEEE Trans. Geoscience & Remote Sensing*, vol. 42, no. 11, pp. 2370-2384, Nov. 2004.

[2] L. Pralon, B. Pompeo, J.M. Fortes, "Stochastic analysis of random frequency modulated waveforms for noise radar systems," *IEEE Trans. Aerospace & Electronic Systems*, vol. 51, no. 2, pp. 1447-1461, Apr. 2015.

[3] S.D. Blunt, et al., "Principles & applications of random FM radar waveform design," *IEEE Aerospace & Electronic Systems Mag*., vol. 35, no. 10, pp. 20-28, Oct. 2020.

[4] M. Heintzelman, J.W. Owen, S.D. Blunt, B. Maio, E. Steinbach, "Practical considerations for optimal mismatched filtering of nonrepeating waveforms," *IEEE Radar Conf.*, San Antonio, TX, May 2023.

[5] J. Jakabosky, S.D. Blunt, B. Himed, "Spectral-shaped optimized FM noise radar for pulse agility," *IEEE Radar Conf.*, Philadelphia, PA, May 2016.

[6] C. Mohr, P.M. McCormick, S.D. Blunt, C. Mott, "Spectrally-efficient FM noise radar waveforms optimized in the logarithmic domain," *IEEE Radar Conf.*, Oklahoma City, OK, Apr. 2018.

[7] C. Mohr, S.D. Blunt, "FM noise waveforms optimized according to a temporal template error (TTE) metric," *IEEE Radar Conf.*, Boston, MA, Apr. 2019.

[8] C.A. Mohr, S.D. Blunt, "Design and generation of stochastically defined pulsed FM noise waveforms", *Intl. Radar Conf.*, Toulon, France, Sept. 2019.

[9] E.R. Biehl, C.A. Mohr, B. Ravenscroft, S.D. Blunt, "Assessment of constant envelope OFDM as a class of random FM radar waveforms", *IEEE Radar Conf*., Florence, Italy, Sept. 2020.

[10] T.J. Kramer, E.R. Biehl, M.B. Heintzelman, S.D. Blunt, E.D. Steinbach, "Compact parameterization of nonrepeating FMCW radar waveforms," *IEEE Radar Conf*., San Antonio, TX, May 2023.

[11] T.J. Kramer, M.B. Heintzelman, S.D. Blunt, "On the repeated use of random FM waveforms", *IEEE Radar Conf*., New York City, NY, Mar. 2022

[12] J.P. Costas, "A study of a class of detection waveforms having nearly idedal range-Doppler ambiguity properties," *Proc. IEEE*, vol. 72, no. 8, pp. 996-1009, Aug. 1984.

[13] J.A. LeMieux, F.M. Ingels, "Analysis of FSK/PSK modulated radar signals using Costas arrayss and complementary welti codes," *IEEE Intl. Radar Conf*., Arlington, VA, May 1990.

[14] C. Chang, M.R. Bell, "Frequency-coded waveforms for enchanced delay-Doppler resolution," *IEEE Trans. Info. Theory*, vol. 49, no. 11, pp. 2960-2971, Nov. 2003.

[15] J.K. Beard, K. Erickson, M. Monteleone, M. Wright, J.C. Russo, "Combinatoric collaboration on Costas arrays and radar applications," *IEEE Radar Conf*., Philidelphia, PA, Apr. 2004.

[16] Z.A. Wagner, D.A. Garen, P.E. Pace, "SAR imagery via frequency shift keying Costas coding," *IEEE Radar Conf*., Seattle, WA, May 2017.

[17] B. Correll, "More new structural properties of Costas arrays," *IEEE Radar Conf*., Boston, MA, Apr. 2019.

[18] N. Neuberger, R. Vehmas, "A Costas-based waveform for local range-Doppler sidelobe level reduction," *IEEE Signal Processing Letters*, vol. 28, pp. 673-677, Mar. 2021.

[19] R.M. Narayanan, T.D. Bufler, B. Leshchinskiy, "Radar ambiguity functions and resolution characteristics of sudoku-based waveforms," *IEEE Radar Conf*., Philadelphia, PA, May 2016.

[20] R. Senanayake, P. Smith, J. Evans, B. Moran, R.J. Evans, "A novel joint radar and communications technique based on frequency permutations," *IEEE Vehicular Technology Conf*., Norman, OK, Sept. 2021.

[21] W. Wang, "MIMO SAR chirp modulation diversity waveform design," *IEEE Geoscience & Remote Sensing Letters*, Vol. 11, No. 9, pp. 1644-1648, Feb. 2014.

[22] H. Sun, F. Brigui, M. Lesturgie, "Analysis and comparison of MIMO radar waveforms," *Intl. Radar Conf*., Lille, France, Oct. 2014.

[23] H. Chahrour, S. Rajan, R. Dansereau, B. Balaji, "Hybrid spread spectrum orthoganal waveforms for MIMO radar," *IEEE Radar Conf*., Oklahoma City, OK, Apr. 2018.

[24] Y. Pailhas, Y. Petillot, "Wideband CDMA waveforms for large MIMO sonar systems," *Sensor Signal Processing for Defense Conf*., Edinburgh, UK, Sept. 2015.

[25] S.D. Blunt, M. Cook, J. Jakabosky, J. de Graaf, E. Perrins, "Polyphase-coded FM (PCFM) radar waveforms, part I: implementation," *IEEE Trans. Aerospace & Electronic Systems*, vol. 50, no. 3, pp. 2218-2229, July 2014.

[26] N. Levanon, E. Mozeson, *Radar Signals*, Wiley-IEEE Press, 2004.

[27] T. Kramer, S.D. Blunt, "Time-frequency analysis of spectrally-notched random FM waveforms," *IEEE Intl. Radar Conf*., Washington, DC, Apr. 2020.